NOTES AND CORRESPONDENCE

Two Limiting Types of Oceanic Finestructures

JOSÉ OCHOA

Centro de Investigación Científica y de Educación Superior de Ensenada, Baja California, México

29 September 1986 and 27 February 1987

ABSTRACT

Profiles from CTD surveys in the Northeastern Pacific are used to study temperature, salinity and density finestructures. Finestructures are defined here as those perturbations of the thermodynamic fields which are not due to internal wave advection and whose vertical extent is between 1 and 100 m. It is shown that two limiting types of finestructures can be distinctly identified: step-structures and intrusions. A step-structure could be the signature of a mixing event; the temperature versus salinity (T–S) relationship is almost linear and the vertical configuration shows a weakly stratified layer bounded above and below by highly stratified but relatively thin regions. An intrusion is the result of lateral interleaving when the displaced water is of different type than the intruding one and their densities are practically the same. The difference in water types could be so large that the intrusion is warmer and saltier, or colder and fresher than its neighbors above and below. In this limit, density increases smoothly with depth, and sudden changes of temperature and salinity occur simultaneously in a density compensating way. Therefore, the T–S relationship is nonlinear and shows cusps in the direction of isopycnals.

These two processes result in a perfect correlation between the temperature and salinity contributions to the buoyancy frequency squared. It is +1 when only step-structures show up, and −1 when only intrusions do. This note shows that in the area of the observations some vertical ranges are populated mainly by one or the other limiting type, implying a differential strength in the finestructure producing processes.

1. Introduction

The information provided by CTD surveys is suitable to the study of finestructures. The distributions of temperature and salinity in the ocean, superimposed on a background of larger spatial scale, have distinct deviations with vertical extent between 1 and 100 meters. Here the term finestructures is used for deviations in this background which are not wave-induced perturbations, corresponding to what Desaubies and Gregg (1981) call irreversible finestructures. Reviews by Fedorov (1978), Gregg and Briscoe (1979), Turner (1981) and Munk (1981) give a general picture of ideas and definitions, recent and historical developments, and the association with processes in other scales.

This note presents observations in which a clear statistical distinction between step-structures and intrusions is shown. The observations show that finestructures appear in two limiting forms—step-structures and intrusions—illustrated in Fig. 1, and that some depth ranges are mainly populated by one or the other type. A step-structure is the combination of a layer bounded above and below by sheets. In comparison with the overall spatial distribution, the layer is weakly stratified and the sheets are highly stratified. A step-structure could be the signature left by a mixing event inside a region that originally was smoothly stratified both in temperature and in salinity. The T–S relationship remains unchanged in the case of such mixing, but the vertical distributions of thermal properties change dramatically. Intrusions are the signature of interleaving or other lateral processes along isopycnals, since mixing or advection in the vertical cannot produce them. This signature of interleaving only occurs when waters of different types are involved. Interleaving does not produce intrusions if a unique linear T–S relationship (a single water mass) exists throughout the region. Only when the displaced waters are of different types than those originally present does interleaving produce intrusions. They are commonly observed in the vicinity of oceanic fronts (Joyce et al., 1978; Georgi, 1978; Gregg, 1980). Often the interleaving is with waters of such a high contrast of thermal properties that intrusions are warmer and saltier, or colder and fresher than their neighbors above and below, but with potential density increasing smoothly with depth.

Since each type of finestructure indicates different processes it is important and useful to distinguish and quantify them. The distribution of finestructures shown in this note is evidence of a remarkable differential strength in such finestructure producing processes. Notice that vertical mixing destroys intrusions in a somehow diffusive way.

Throughout this paper a way of comparing the temperature and salinity vertical gradients is required. This can be done by considering their respective contributions to the buoyancy frequency squared (N^2). The buoyancy frequency indicates the intensity of density

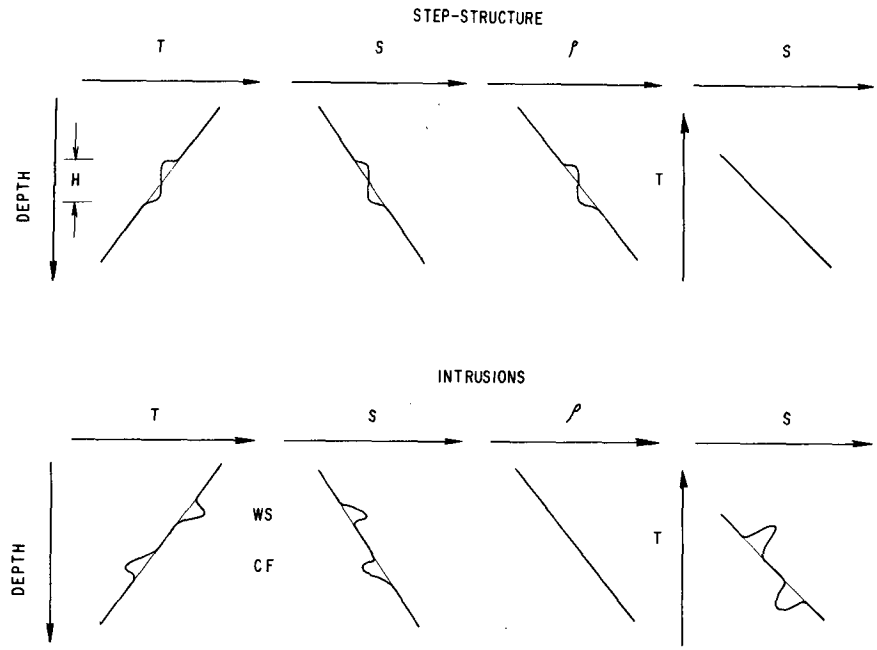

FIG. 1. Schematic representation of two limiting types of oceanic finestructures. (i) Step-structures consist of thick, weakly stratified regions or layers bounded above and below by thin, highly stratified regions or sheets. The T–S relationship is almost linear. They could be thought of as the signature left by mixing events in regions where temperature and salinity were originally smoothly stratified. (ii) An intrusion is the signature of lateral (along-isopycnal) interleaving, when the intruding water is of a different type than the displaced water. Density remains smoothly stratified and the differences in water types could be so large as to produce inversions in the temperature or salinity vertical distributions. There are warm salty (WS) and cold fresh (CF) intrusions. The T–S relationship shows cusps aligned in the direction of isopycnals.

stratification once the effect of adiabatic compressibility is removed. The expression for the buoyancy frequency squared is

$$N^2 = -g\rho^{-1}\partial\rho/\partial z - g^2c^{-2} \quad (1)$$

where g is gravity, ρ is density, z is the vertical coordinate (positive upwards) and c is the speed of sound. The equivalent expression in terms of temperature (T) and salinity (S) is

$$N^2 = g\alpha(\partial T/\partial z - \rho g\Delta) - g\beta\partial S/\partial z \quad (2)$$

where α is the coefficient of thermal expansion, Δ the adiabatic lapse rate and β the coefficient of haline contraction. From this expression one can distinguish the individual contributions to the buoyancy frequency squared, namely,

$$N_T^2 = g\alpha(\partial T/\partial z - \rho g\Delta), \quad (3)$$

$$N_S^2 = -g\beta\partial S/\partial z. \quad (4)$$

Neglecting diffusion, the stability of the static state is guaranteed if N^2 is positive. Negative measurements of N^2 indicate heavier waters overlying lighter ones, a result of overturning events. Even when N^2 is positive the differential diffusion of heat, salt and momentum allows instabilities when either N_T^2 is negative (diffusive regime) or N_S^2 is negative (salt finger regime)—these are the double diffusive phenomena. Expressions (3) and (4) can be used to indicate where, which and how intense double diffusive phenomena are (Ruddick, 1983; Turner, 1981; Walin, 1964). In Figs. 4 and 7, vertical distributions illustrate these definitions.

In this note it will be shown that, for the region of the observations where the vertical averages of N_T^2 and N_S^2 are positive, the correlation between N_T^2 and N_S^2 approaches the two limits of perfect correlation (+1 and −1). When step-structures dominate, temperature and salinity contributions to the buoyancy frequency squared are positive and nearly proportional. Therefore, the correlation is close to +1. The other limit is approached when intrusions dominate. In a region populated with intense intrusions, the vertical profiles of N_T^2 and N_S^2 look like mirror images; a negative contribution from either one is compensated by the other, such that the total buoyancy frequency squared is positive (Fig. 5). This association of relative maxima (minima) of one contribution with relative minima (maxima) of the other produces a correlation coefficient close to −1.

2. Observations

The measurements were obtained with a Neil Brown Mark III CTD having a sampling rate of 30 Hz. The

first step to process the data consisted in smoothing the three time series, the combined fast thermistor and platinum resistance temperature series, the conductivity series and the pressure series. The smoothing was done with a recursive first-order Butterworth filter (Otnes and Enochson, 1978). The convolution was carried forward and backward in time, so the total phase shift is null. Finally, salinity spiking was observed to be reduced by computing salinity with lagged conductivity values. In this dataset the best lag (visually checked) was two scans (66 ms).

The smoothing in the temperature and conductivity series is such that the amplitude of sinusoidal variations with vertical wavelengths of 1, 2 and 10 m have been attenuated to 4%, 13% and 80%, respectively. Subsampling for cross-spectral analysis was done with higher resolution than 1 m to minimize aliasing, but it is clear that the limit of credibility is between 2 and 1 m, certainly not higher, wavenumbers. The statistical results shown are coherences and should not be influenced by such attenuation provided proper care is taken with "leaking," as is the case with the prewhitening performed.

The series of CTD measurements were obtained during the spring of 1978 about 300 km west of Ensenada, Mexico (near 30°30'N, 120°35'W) aboard the R/V *Wecoma*. The data are from two sets of measurements. For the first set of observations, three stations at the vertices of an equilateral triangle of 9.6 km per side were occupied cyclically. Thirteen cycles were completed, with all casts made to a depth of 1500 m. The total time span was 53 hours, thus covering two inertial periods. Data from the depth range between 140 and 240 db are shown and are used to compute the statistics. In this depth range the T–S relationship is almost linear (Fig. 2) and the overall vertical temperature gradient is about 0.02°C m^{-1}.

The second set of measurements consists of 38 cycles of tow-yo (this is lowering and raising the CTD while the ship tows it) covering the depth range betweeen 500 and 600 db. The towing speed was nominally 0.77 m s^{-1} (1.5 kt). The lowering and raising rate was 1 m s^{-1}, hence the zig-zag pattern in the vertical plane repeats itself every 150 m. Since, for a given distance, variations of properties in the horizontal are considerably smaller than in the vertical, the estimation of the vertical gradients neglected horizontal variations. The T–S relationship for this depth range forms a zig-zag pattern (Fig. 2) and the overall vertical temperature gradient is about 0.005°C m^{-1} (four times smaller than the other depth range used). In both depth ranges the along-isopycnal gradient of thermal properties is, as shown in Fig. 2, about the same 0.01°C km^{-1}, hence lateral interleaving is equally efficient in producing intrusions. The existence of this lateral (along-isopycnal) gradient is crucial since otherwise interleaving cannot be identified from hydrographic data.

The expected errors in N_T^2 and N_S^2 are not directly known but using the results of Gregg (1979) and taking in account the smoothing effects, an estimate of errors in N^2 can be shown. The vertical separation for the computation of vertical gradients is 1 m. Gregg (1979) estimates that for this separation (assuming no time response mismatch, see his Fig. 12), the noise level when $N = 2.5$ cph, which is the mean value in the 500–600 db range, is 50%, a rather low signal-to-noise ratio, especially considering that for lower N values the error is larger. The noise level increases as the vertical interval in which the estimate is done decreases, and decreases as the actual value of the estimate increases. This estimate is computed assuming that the only noise is the quantization noise in the temperature, conductivity and pressure series. The smoothing performed reduces the variance of white noise by two orders of magnitude,

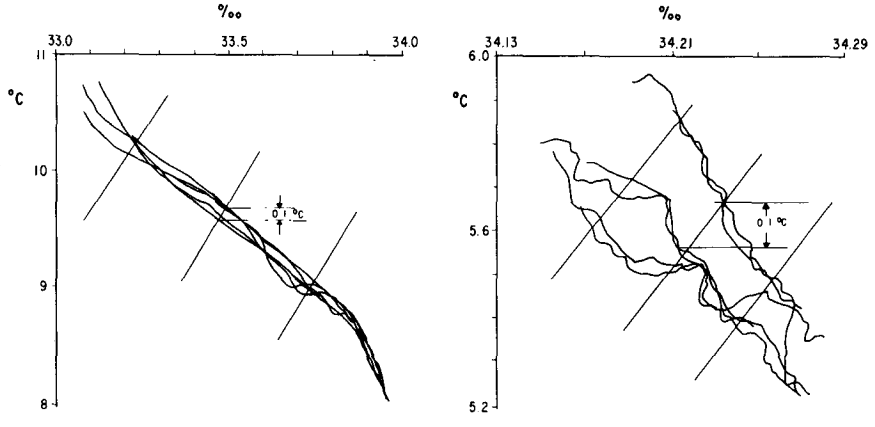

FIG. 2. T–S relationship of the first two cycles in the 9.6 km triangular array. In both depth ranges the contrast of thermal properties along isopycnals is about the same (0.01°C km^{-1}). The smoothness in the shallower region differs substantially with the irregular zig-zag pattern of the deeper range.

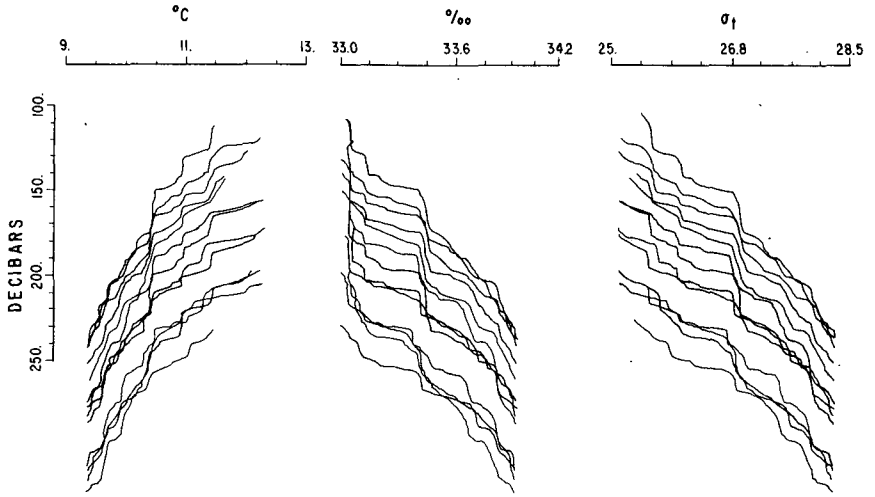

FIG. 3. Thirteen sets of temperature, salinity and σ_t at one of the vertices in the triangular array. The depth shown overlaps the range used for computing statistics. Each set of profiles is displaced 9 db from the previous one (see text).

which in terms of Eqs. (30) and (31) given by Gregg (1979), implies a decrease of one order of magnitude in the noise level. Therefore, in the smoothed data, there is a noise level of 5% or less for values of $N > 2.5$ cph. In essence, the result of the smoothing performed is equivalent to estimates on a larger vertical interval, implying high signal-to-noise ratios. For the region between 140 and 240 db the perspective is better since there are less values with $N < 2.5$ cph. A consequence of the smoothing is the loss of vertical resolution, and coherences at vertical wavenumbers higher than 0.5 cpm should be considered with caution.

3. Results and discussion

In the triangular array experiment, configurations resembling staircases were observed in temperature, salinity and density (σ_t); see Fig. 3. Double diffusive processes in the vertical are not acting since both temperature (N_T^2) and salinity (N_S^2) contributions to the total buoyancy frequency squared (N^2) are positive. Figure 4 shows vertical profiles of temperature, N_T^2, salinity (‰), N_S^2, σ_t and N^2. Notice that there is the possibility of small N^2 variations resulting from large but compensating variations of N_T^2 and N_S^2; such variations are negligible in this depth range. In the depth range shown, N^2 is always larger and almost directly proportional to either N_T^2 or N_S^2. This is a consequence of the almost linear T–S relationship.

Internal waves produce transient distortions of the "internal wave free" distributions, which are called reversible finestructures by Desaubies and Gregg (1981). The persistence of the step-structures (as shown in Fig. 3) over periods longer than two inertial periods rules them out as reversible finestructures. Notice that the weakly stratified regions are squeezed, stretched, and

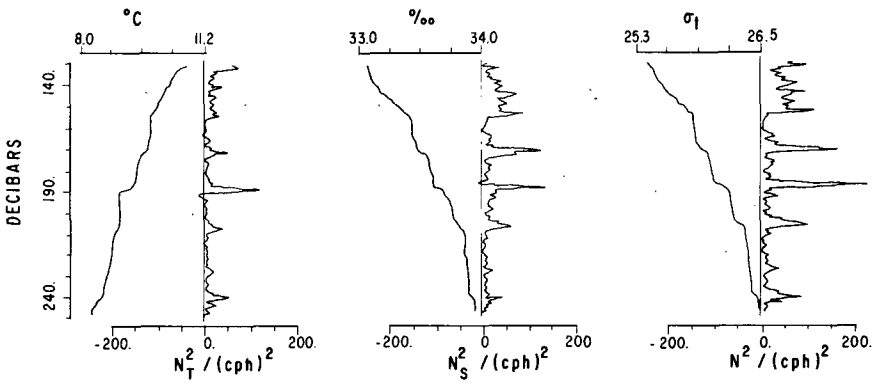

FIG. 4. A section of the vertical distribution of temperature (°C), N_T^2, salinity (‰), N_S^2, σ_t and N^2 for one of the stations in the triangular array described in the text. Here, N_T^2 and N_S^2 are positive and add constructively.

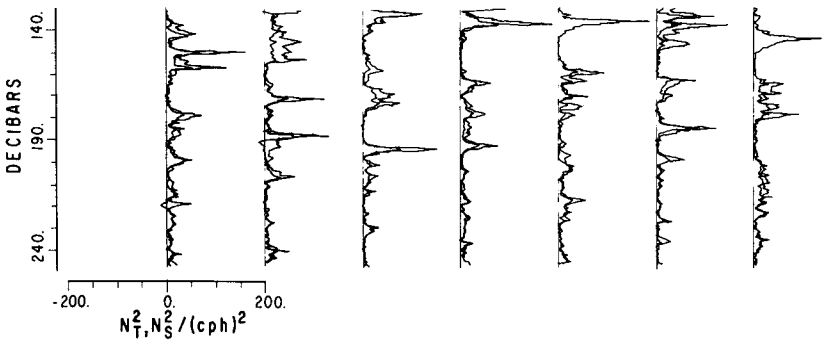

FIG. 5. Vertical distribution of N_T^2 and N_S^2 for the first eight casts in the triangular array. The second pair corresponds to the profiles shown in Fig. 4. Notice that they are almost proportional.

moved up and down, but they do not propagate from their density level. Most of these wiggles are not propagating features. They should be considered part of the "internal wave free" distributions and classified as irreversible finestructures.

The correlation between N_T^2 and N_S^2 is almost perfect, as illustrated by Fig. 5. The coherence between N_T^2 and N_S^2 as a function of vertical wavenumber is shown in Fig. 6. Coherences were computed from ensemble averaged Fourier transforms (Haubrich, 1965). The original profiles were first differenced and a Bartlett window was applied before Fourier transforming. Fundamental bands were not averaged. The correlation is high throughout the whole vertical wavenumber band, and the near zero phase indicates the vertical alignment. The 95% confidence level for null coherence shown in Fig. 5 was computed using the vertical profiles as if they were statistically independent, which in view of the persistency of the structures (Fig. 3) is not true. Therefore, an unbiased estimate of the 95% confidence level should be above the one shown. Nevertheless, notice that band averaging will not modify the near zero phase.

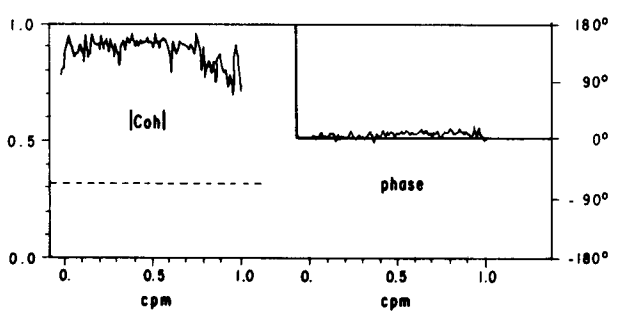

FIG. 6. Coherence between N_T^2 and N_S^2 is plotted as a function of vertical wavenumber. The ensemble average includes 76 pairs. The coherence is high because N_T^2 and N_S^2 are nearly proportional. The near zero phase lag is a consequence of the alignment between N_T^2 and N_S^2 vertical variations. The 95% confidence limit for null coherence is indicated by the dashed line.

From the tow-yo measurements in the depth range 500–600 db, the simple picture of steps is blurred with an enrichment of finestructures (Fig. 7). Although negative contributions from either N_T^2 or N_S^2 are present, N^2 is positive, indicating the absence of overturning events. These negative contributions are associated with inversions from the overall temperature and salinity distributions and characterize intrusive features. Their spatial scales had been studied by Georgi (1978) and Gregg (1980).

Figure 7 shows the first profile from a set of 76 in the same way as Fig. 4. Double diffusive processes in the vertical can occur in regions where either N_T^2 (diffusive regime) or N_S^2 (salt finger regime) are negative. When N_T^2 and N_S^2 are plotted against the same axis (Fig. 8) their high correlation is readily seen. Unlike the case of step-structures where N_T^2 and N_S^2 are positive and almost proportional, the correlation in the presence of strong intrusive features is of the opposite sign. In this case, relative maxima (minima) of one coincide with minima (maxima) of the other. This high correlation and mirrorlike appearance translate into high coherence and phase lag of 180° in vertical wavenumber space. Figure 9 shows the computed coherence and the phase lag. The latter is close but consistently less than 180°, indicating that temperature structures are slightly deeper than salinity structures. In the upper frame of Fig. 9 the coherence was computed with profiles (38) obtained while the CTD was descending. In the other frame the coherence was computed with profiles (38) obtained while the CTD was ascending. Therefore, the result of a phase lag of 180° is not dependent on instrumental errors (mismatch in temperature–conductivity response times) since the same tendency is shown in up and down profiles. Contiguous profiles are correlated in the low wavenumber region, and the number of degrees of freedom are again not as high as estimated when deriving the 95% confidence level for the null coherence shown (the dashed line in Figs. 6 and 9 is an optimistic estimate of the 95% confidence level). Again, further band averaging will not modify the important result of the phase lag.

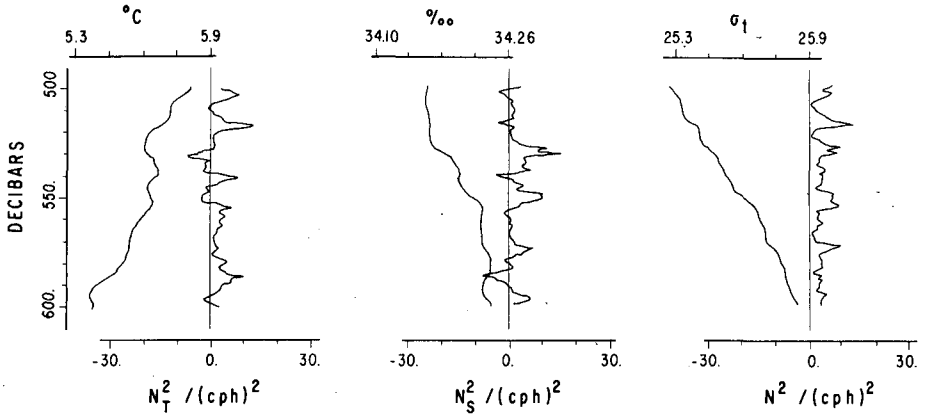

FIG. 7. Data from the first descending trip during the tow-yo (compare with Fig. 4). There are regions where the temperature (salinity) contribution to the buoyancy frequency squared is negative, but the salinity (temperature) contribution compensates such that the total buoyancy frequency squared is positive throughout the depth shown.

The same depth range between 500 and 600 db was analyzed in the data of the triangular array previously described, with the same results as the ones shown here. The phase close to 180° for the two subsets of profiles (up and down) is shown because it is strong evidence that the problem of salinity spiking (a more serious problem than system noise) is not affecting the result.

In a study focused on interleaving, Joyce et al. (1978) have computed the coherence between temperature and salinity vertical gradients, showing high coherence and almost exact 0° phase lag for wavelengths longer than 4 m (their Fig. 17). This result corresponds to 180° phase lag in terms of the temperature and salinity contributions to the buoyancy frequency squared because of the opposite signs between N_S^2 and $\partial S/\partial z$.

In regions where the overall T–S relationship is such that the vertical average of either N_T^2 or N_S^2 is negative, mixing events produce vertical distributions of N_T^2 and N_S^2 that look like mirror images. Under these circumstances both mixing events and lateral interleaving produce a correlation coefficient close to −1. In such regions this kind of analysis does not produce the results shown here.

In conclusion, there are regions mainly populated by one or the other characteristic type of irreversible finestructures, and this is shown with a simple and specific statistical result. For the data used here, the depth range between 140 and 240 db shows high coherence between N_T^2 and N_S^2 with almost 0° of phase lag (hence, +1 correlation) because almost pure step-structures are present. The depth range between 500 and 600 db also shows high coherence but a phase lag close to 180° (hence, −1 correlation) because intrusions dominate.

Interleaving is equally efficient producing intrusions in both depth ranges because of the same along-isopycnal water contrasts (Fig. 2). Mixing in the vertical builds up step-structures and diffuses away intrusions

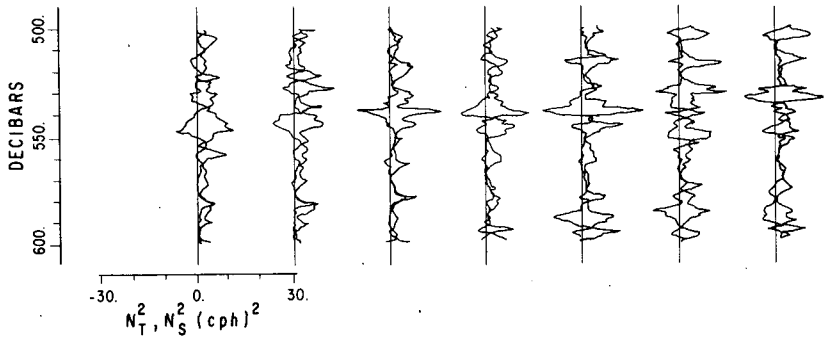

FIG. 8. Vertical distribution of N_T^2 and N_S^2 for the first seven descending trips during the tow-yo. Relative maxima in one quantity coincide with relative minima in the other, producing a mirrorlike pairing. The relative maxima that occur in the first three pairs around 580 db are exceptions to this mirrorlike appearance. Each pair is 300 m horizontally apart.

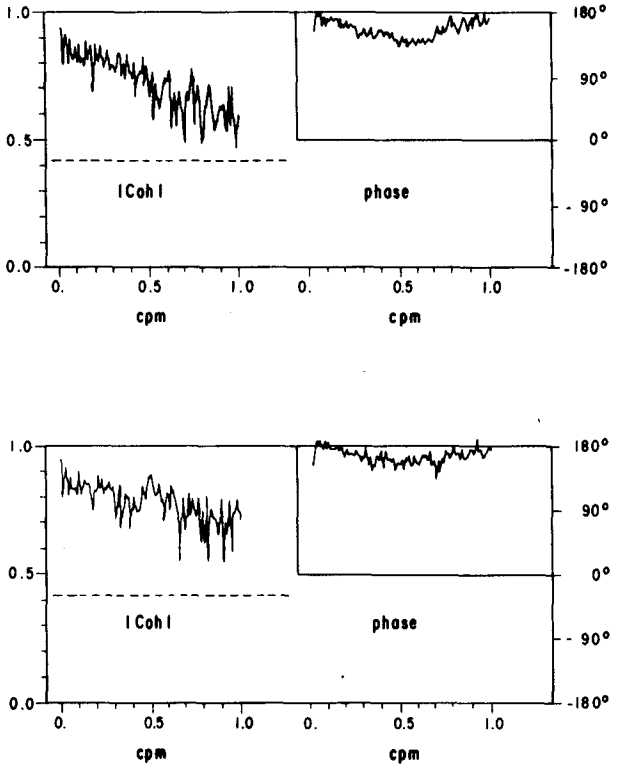

FIG. 9. Coherence between N_T^2 and N_S^2 for the data of the tow-yo. The high coherence and phase lag around 180° is a consequence of the mirrorlike pairing. The 95% confidence limit for null coherence is indicated by the dashed line (see text).

if present. Uniform existence of both processes should cause certain balance in the distribution of the two types of finestructures. An explanation of the surprising domination of one type of finestructure in either depth range could be due to differential strength of vertical mixing and interleaving in each range. This analysis shows evidence supporting that the interleaving is weak in comparison with the vertical mixing for the shallower region and vice versa for the deeper region.

Acknowledgments. This work is part of my doctoral dissertation. I thank Charles S. Cox for his guidance and for providing me with the data. Also, I thank Pedro Ripa, Libe Washburn and Antoine Badan for helpful criticism. The figures were done by Sergio Ramos and Fabian Cabrera. I am grateful to the Mexican National Council of Science and Technology (CONACYT) for the funding provided during my graduate studies.

REFERENCES

Desaubies, Y., and M. C. Gregg, 1981: Reversible and irreversible finestructure. *J. Phys. Oceanogr.*, **11,** 541–556.

Federov, K. N., 1978: *The Thermohaline Finestructure of the Oceans,* Pergamon Press, 170 pp.

Georgi, D., 1978: Finestructure in the Antarctic polar front zone: Its characteristics and possible relationship to internal waves. *J. Geophys. Res.*, **83,** 4579–4588.

Gregg, M. C., 1979: The effects of bias errors and system noise on parameters computed from C, T, P and V profiles. *J. Phys. Oceanogr.*, **9,** 199–217.

——, 1980: The three-dimensional mapping of a small thermohaline intrusion. *J. Phys. Oceanogr.*, **10,** 1468–1492.

——, and M. G. Briscoe, 1979: Internal waves, finestructure and mixing in the ocean. *Rev. Geophys. Space Phys.*, **17,** 1524–1548.

Haubrich, R. A., 1965: Earth noise, 5 to 500 millicycles per second. *J. Geophys. Res.*, **70,** 1415–1427.

Joyce, T. M., W. Zenk and J. M. Toole, 1978: The anatomy of the Antarctic polar front in the Drake Passage. *J. Geophys. Res.*, **83,** 6093–6114.

Munk, W., 1981: Internal waves and small-scale processes, 8. *Evolution of Physical Oceanography,* B. A. Warren and C. Wunch, Eds., MIT Press, 264–291.

Otnes, R. K., and L. Enochson, 1978: *Applied Time Series Analysis. Vol. 1,* Wiley-Interscience, 449 pp.

Ruddick, B. R., 1983: A practical indicator of the stability of the water column to double-diffusive activity. *Deep-Sea Res.*, **30,** 1105–1107.

Turner, J. S., 1981: Small-scale mixing processes, 9. *Evolution of Physical Oceanography,* B. A. Warren and C. Wunch, Eds., MIT Press, 236–262.

Walin, G., 1964: Note on the stability of water stratified by both salt and heat. *Tellus,* **16,** 389–393.